Coastal Survey of archaeological sites using drones

Skarlatos D., Savvidou E.

Cyprus University of Technology, 30 Archbishop Kyprianou Str., 3036 Limassol, Cyprus. +357 25002360

1. Introduction

Cultural Heritage should be documented and preserved in order to be inherited to future generations. With climate change and sea level rise, archaeological monuments situated at the shoreline or submerged to various depths under the sea surface are gradually shifting with the risk of damage or even disappearance. Especially in the Mediterranean waters, where a wealth of monuments exists, the situation is even more crucial. Geometric documentation is therefore extremely critical in the case of submerge monuments.

Although photogrammetry has become a widely acceptable tool for the geometric documentation of inland archaeological sites and monuments inland with increased accuracy and minimal processing times, methods for documenting submerged archaeological sites, especially in shallow waters, are insufficient, while the use of traditional methods is impossible or inefficient.

In case of shallow waters, application of the two media photogrammetric technique, where the camera is located above sea surface (air) and the object being photographed is submerged (water), has been reported by many (Karara, 1972; Slama, 1980; Shan, 1994), with the basic optical principles proving that photogrammetric processing through water is possible. In most cases a special platform is used for hoisting the camera (Whittlesey 1975; Fryer 1983; Westaway et al. 2001; Georgopoulos and Agrafiotis 2012), and a methodology was adopted to correct the photos from the refraction effect at the water surface. Georgopoulos and Agrafiotis (2012) documented a submerged monument at a depth of 0.5 to 2 meters establishing a 3-point network ashore in order to enable control point measurements.

In order to perform photogrammetric procedures a simple algorithm was developed to correct the images from the refraction effect. The algorithm takes as input the depth of all imaged points, the height of the camera and the refractive index, as well as the camera constant in pixels and the coordinates of the principal point. The algorithm then calculates the radial distance of each pixel from the principal point and reads the depth from the relevant table, and determines the new corrected radial distance. A corrected image is then gradually constructed using the corrected radial distances resulting in a new image of the same resolution and dimension as the initial one. On the corrected image the objects occupy a smaller area due to the refraction geometry (Georgopoulos and Agrafiotis 2012).

Aerial imagery has also been used for mapping areas with clear waters and shallow depths (5-10m). Masry (1975) developed a method for correcting refraction using the analytical plotter model AP/2C, an instrument that combines the advantages of both the analytical and analogue methods in the analytical plotter. All parameters pertaining to the photography (e.g. camera altitude, imaging rays, principal point, etc.) are digitally represented in the computer and are continuously used by the control program calculating the photographs positions' in the viewer, thus maintaining the stereo-model. In these calculations, the refraction effect can be included.

The method was applied and tested on two stereo models with land coverage of 50% of the total overlap between the two images. The images were collected at 38 meters flying height with a 1/10000 scale. The models were corrected and depth measurements of spot heights were carried out and compared with depth surroundings. A 10% approximate accuracy of the water depth was achieved with the root mean square error of all depth points in the two models tested to be 0.45m (Masry 1975).

The aim of this project is to develop new methods for mapping and detection of coastal archaeological sites using technologies such as Autonomous Unmanned Aerial Vehicles (AUAV or drones), that have recently become affordable. Image Based Methods (IBM) such as Structure from Motion (SfM) and Multi View Stereo (MVS) for 3D recording and documentation are becoming more popular as a result of improved image processing algorithms, while impressive level of detail and precision is attained. Therefore, the use of fixed wing AUAVs and multicopters for 3D mapping and orthophotos production is nowadays widely recognized and has become accepted as a standard tool for archaeological site documentation or excavation progress monitoring, although there are still limitations and constrains.

The need for such investigation has been raised during discussions with MARELab of the Archaeological Research Unit of the Cyprus University, regarding ways to survey coastal sites. During September 2012, in collaboration with NAS and MARELab, sparse positions of some anchorages at an ancient anchorage coastal site were collected using a dual frequency GPS as handheld devices over buoys. This method proven to be not an easy nor a productive task, while the final output was a sparse point layer with find's positions and depth over an otherwise blank map with main feature the coast line. The difficulties, inaccuracies and survey quality of coastal site recording, lead to the decision to further investigate the UAV possibilities of coastal mapping.

Orthophotomosaics are precise and georeferenced maps created by seamlessly mosaicked orthorectified densely overlapping aerial photos. The extended use of UAVs and drones along with software automations, facilitated their wide adoption as mapping tools for archaeological aerial surveys as they can provide much more visual information and if used as a backdrop to existing geo information, can help interpretation and understanding of the relationship among finds in a context rich map. Especially in coastal sites where there is the need to relate both overwater structures with underwater ones or finds, the use of seamless orthophotomaps, which reveal visual information of both sea bottom and ground structures, could be an invaluable tool. Since aerial imagery may penetrate more than 13m in clear Meditteranean water, coastal archaeological sites could also be benefited by mapping and monitoring using similar techniques and products.

Orthophotomosaics however cannot be used in submerged coastal zones as their processing is not trivial; the straight rays of light are refracted in sea surface affecting both the 3D bathymetric model as well as final orthophotomosaic accuracy.

The aim of this project is to address these problems by proposing new methods and algorithms, integrating both land and shallow water underwater orthophotos in a seamless and precise orthophotomosaic, thus providing means to gather reliable information both for documentation and analysis, bypassing the tedious task of single point GPS measurements. These tools will assist local archaeological research in

Cyprus, for sites such as ancient Paphos, Amathounta ancient harbor and Agia Napa anchorage site.

2. Methodology

The objective is to streamline the process of creating bathymetric contours, orthophotomosaics on coastal shallow waters for survey detection, documentation and monitoring of coastal archaeological sites.

The standard process for creating an orthophoto from aerial imagery (fig. 2 – blue rectangles) begins with the import of the photos and the ground control points collected, followed by Structure from Motion (SfM) aerial triangulation and camera self-calibration, to produce a Multi View Stereo (MVS) Digital Surface Model (SDM). Orthophotographs are then created to finally produce an Orthophotomap through the process of mosaicking. The final Orthophotomaps is then exported.

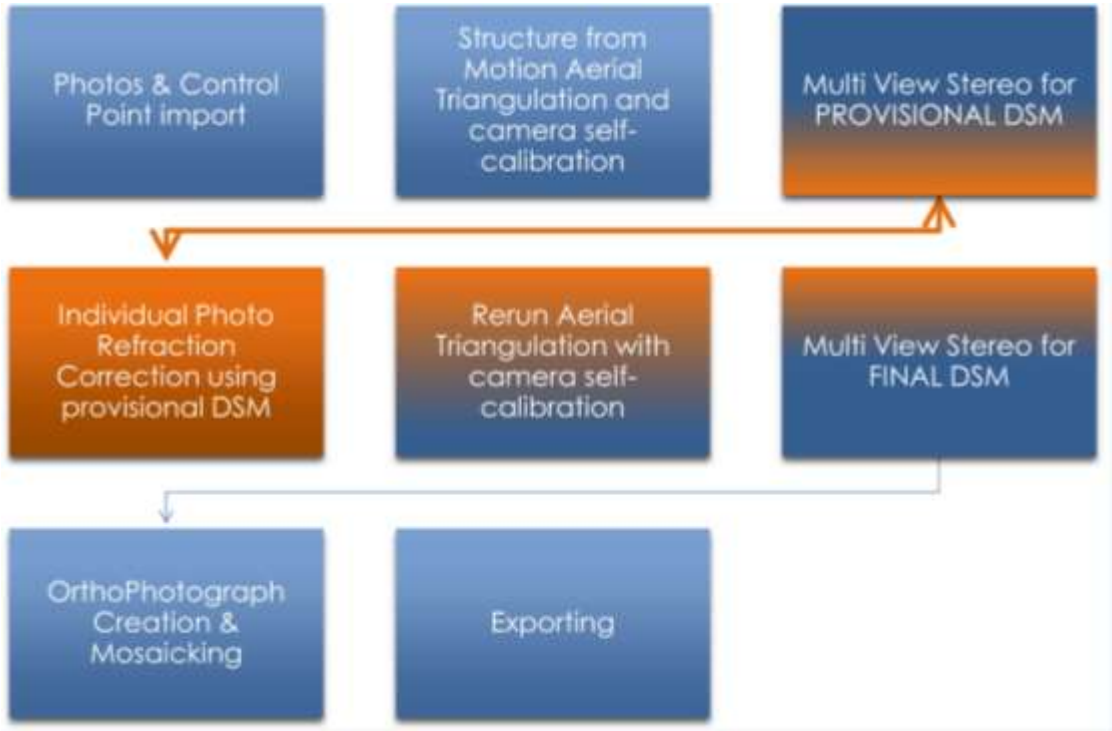

fig. 2 - Proposed methodology for Orthophoto creation corrected from refraction.

The proposed methodology incorporates into the standard process an orthophoto creation methodology (fig. 2 – orange rectangles) that addresses each photo affected from refraction separately, hence producing a seamless Orthophotomap corrected from refraction. Following the standard process, a provisional DSM is produced, which is imported into the algorithm along with the original UAV photos, camera parameters and exterior orientation, producing a new set of photos, partially corrected from refraction. The new photos are used to rerun the aerial triangulation keeping the camera calibration the same, produce a new, more accurate DSM. This iterative process is repeated until the DSM shows no significant change, usually 3-4 times, evaluated with known bathymetric checkpoints. From the final DSM, Orthophotographs are created to finally produce and export the Orthophotomap.

The Iterative Orthophoto Refinement (IOR), was introduced by Norvelle (1994, 1996). Norvelle used an iterative process, where the discrepancies between a pair of

orthophotos were translated in DSM height corrections, which were then used to correct the initial DEM. Theoretically, the orthophoto should be independent from the initial photo. In practice however, orthophotos created from different photos slightly differ. The mathematical model of the height correction was simple, and although approximate, multiple iterations produced promising results. Georgopoulos and Skarlatos (2003) investigated the method further and proposed a precise mathematical model for height corrections in any given positions using orthophotos created from a pair of photos. The proposed method, is based on this idea of iterative corrections.

Dekelia coastal area was chosen for the initial algorithm development and verification prior to any application in archaeological coastal site. Final implementation of the algorithm will take place in Agia Napa ancient anchorage site.

3. Application

3.1 Algorithm Development and Verification

A crucial aspect of this project is the evaluation of the proposed methods. This can only be achieved with proper check data, which are not easy to acquire. Thus, additional care is given on the methods that will be used for verification. The coastal archaeological site of Amathus was chosen for the development and verification of the algorithm.

3.1.1 Amathunta archaeological site

Amathunta archaeological site (fig. 3) is located in Lemesos city, Cyprus. Amathus was one of the most significant ancient kingdoms of Cyprus dating back to 1100 BC, built on the coastal cliffs. The remains of the city's ancient port are today visible underwater. An accurate orthophotomap that includes both the overwater city structures and the underwater harbor could be a significant tool for the archaeological documentation of Amathus ancient city.

The ancient city of Amathus is located on the south coast of Cyprus, about 7 kilometers east of Limassol city. In the surrounding region of Amathus traces of human presence have been identified since the Neolithic Age, however it is not known when the city of Amathus has been founded.

The first discoveries in Amathus were made back during the Frankish period and which included large stone potteries located at the acropolis. The first excavations took place during 1893-1894 directed by British archaeologists, while in 1930 the Swedish mission excavated several ancient tombs. After 1960 and the independence of Cyprus, several rescue and systematic excavation were made by the Department of Antiquities, while since 1975 the Athens French School of Archaeology undertook systematic excavation at the acropolis and other places of Amathus.

The acropolis of Amthus, build on the coastal cliffs, served as a natural fortress and also as an observatory. During the archaic period, the city flourished and developed significant trade relations with the neighboring countries, while a number of Phoenician traders were established there. During the revolt of the Cypriots against the Persians, following the Ionian Revolt in 499 BC, Amathus complied pro-Persian stance, which leading to the siege of the city by the insurgents led by Onisilos. The abolition of Amathus kingdom, like many other city-kingdoms of Cyprus, occurs during the Hellenistic period at 312/311 BC, with the annexation of Cyprus to the Ptolemies state. The acropolis was abandoned and life is concentrated in the lower city of Amathus. The city will experience a transient recovery during the Antonine

and Several periods, but the transition to Christianity in the 4th century AC will find Amathus in decline. Although the city survived the first Arab invasion in the mid-7th century, it seems that it was finally abandoned at the end of the same century.

The most significant sites and monuments of Amathus (fig. 3) include the Sanctuary of Aphrodite at the Acropolis [1], the Roman Forum and the Baths [2], the Palace [3], the Port [4], the Walls, the Necropolis and the Basilicas.

fig. 3 - Overview aerial orthophoto of Amathunta archaeological site

In front of the market, to the south, there was the outer harbor of the city, the ruins of which today are visible underwater. The port was built in the late 4th centur BC by Dimitrios the Conqueror for the defense of the city in a period of conflict with the Ptolemies due to the assertion of power in Cyprus. The life of the port was short as it was quickly covered by sand. Research has shown that between the entrance of the archaeological site to the market and the current road, there was an internal port where ships were towed to be protected from strong winds.

3.1.2 Data collection and processing

Three flights were conducted collecting 182 photos in total, with 3cm image resolution, covering an area of about 0.25km^2. A total of 29 ground control points were collected inland using GPS RTK. Using the standard photogrammetric process, the aerial imagery and GCPs were used for aerial triangulation and an initial

provisional DEM (fig. 4) was created, followed by orthophoto creation and mosaicking to produce an initial orthophotomap (fig. 5) of the area. The GCPs were used to georeferenced the final products, achieving accuracy of 6.3cm (0.65 pix).

fig. 4 - Initial Digital Elevation Model of Amathunta coastal archaeological site.

fig. 5 - Orthophotomap of Amathunta coastal archaeological site created from initial dpeths, with GCPs (yellow triangles) and bathymetric lodar check points (red dots).

More than 5500 Lidar bathymetric measurements were used to evaluate the DSM produced. Depth values corresponding to the Lidar reference depths were extracted from the initial DEM (Z0). A comparison of the two datasets produced 39.5% in depth. The main objective of the algorithm was therefore to minimize that error and produce more accurate DEM and orthophotomap of the area which can be used for documentation and analysis.

The aerial photos and initial DEM, along with the camera calibration parameters and exterior orientation were used to run the algorithm and produce a new set of photos, partially corrected from refraction. The new photos were then used to rerun the aerial triangulation and produce a new, more accurate DEM. This iterative process was repeated three time until the DSM showed no significant change, based on the comparison of extracted DSM depths with the reference Lidar depths at checkpoints. From the final DSM, Orthophotographs were created to produce and export the final Orthophotomap.

3.1.3 Results

The results of the Amathunta case study where the algorithm was developed and verified are summarized in fig. 6, fig. 7 and fig. 8. Fig. 6 shows the scatter diagrams of the corrected depths versus the references Lidar depths at more than 5500 checkpoints, (a) after the initial run that produced the provisional DEM, (b) after the first algorithm iteration, (c) after the second algorithm iteration, and (d) after the 3rd and last iteration. While the pattern of the scatter remains similar for all cases, it is clear that the depth values extracted are improved after each iteration. By the last iteration, the linear fitting between the two dataset is very close to 45 degrees, showing a very good correlation.

A statistical analysis of the comparison between the extracted corrected depths and the reference depths is shown is fig. 7. The mean, standard deviation, error percentage and Root Mean Squared Error (RMS) are presented here, showing the improvement in the depth values extracted from the DEMs after each iteration. The error percentage of the provisional DSM decreased from 39.5% to 15.6% after the first iteration, down to 9.1% after the second iteration, and finally to -1.40% after the third and last iteration. This is also indicated by the decrease in the mean, from 1.07m to 0.08m as well as the decrease in RMS from 1.41m to 0.53m. The standard deviation however, is slightly increased after the first iteration, compared to the provisional DSM, even though all other statistical error indicators are greatly decreased. This is because the spread of the depth values, even though corrected remains the same.

Fig 8, shows the error percentage of the corrected depths extracted from the initial DEM (Z0), after the first iteration (Z1), after the second iteration (Z2) and after the third and last iteration (Z3), for different depths ranges. It can be seen that for depths less than 0.5 m, the error percentage decreases after the first iteration but increases again after the second and third iteration, reaching an error greater than the one calculated even for the provisional DSM depths. For depths between 0.5m and 1m, a similar result is observed. There is a great decrease in error after the first iteration, but the error increases after the second and third iteration. In this case however, although the error increases, it is still much smaller than the error calculated for the provisional DSM depths. The pattern changes for depths greater than 1m, where the error greatly decreases after the first iteration and continues to decrease after the second and third iterations. A greater error decrease is observed as the depths increase.

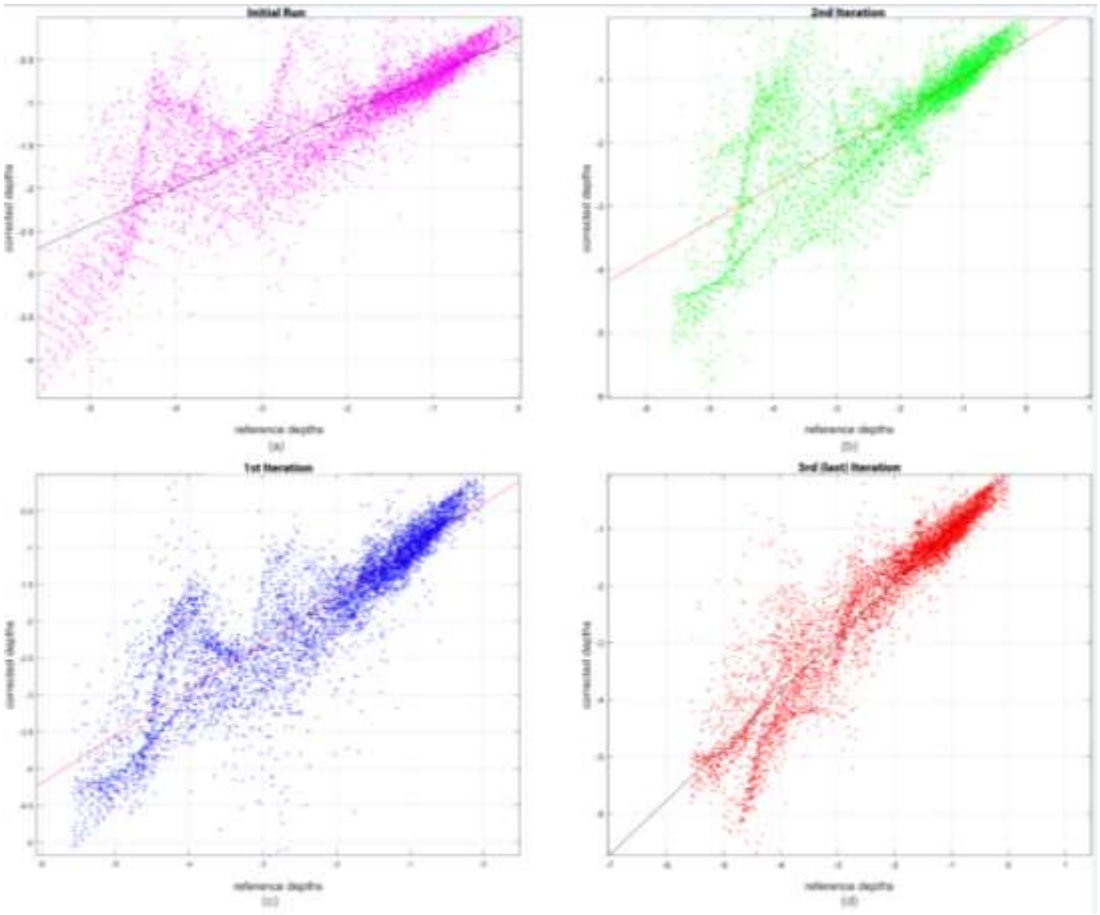

fig. 6 Corrected depths vs. Reference depths at checkpoints (a) after initial run, (b) after 1st iterations, (c) after 2nd iterations and (d) after 3rd (last) iteration.

Iteration	Mean [m]	Standard Deviation [m]	Error Percentage %	RMS [m]
0	1.07	0.92	39.5	1.41
1	0.6	0.93	15.6	1.10
2	0.46	0.74	09.1	0.87
3	0.08	0.53	-1.4	0.53

fig. 7 - Statistics analysis of corrected depths against reference Lidar depths.

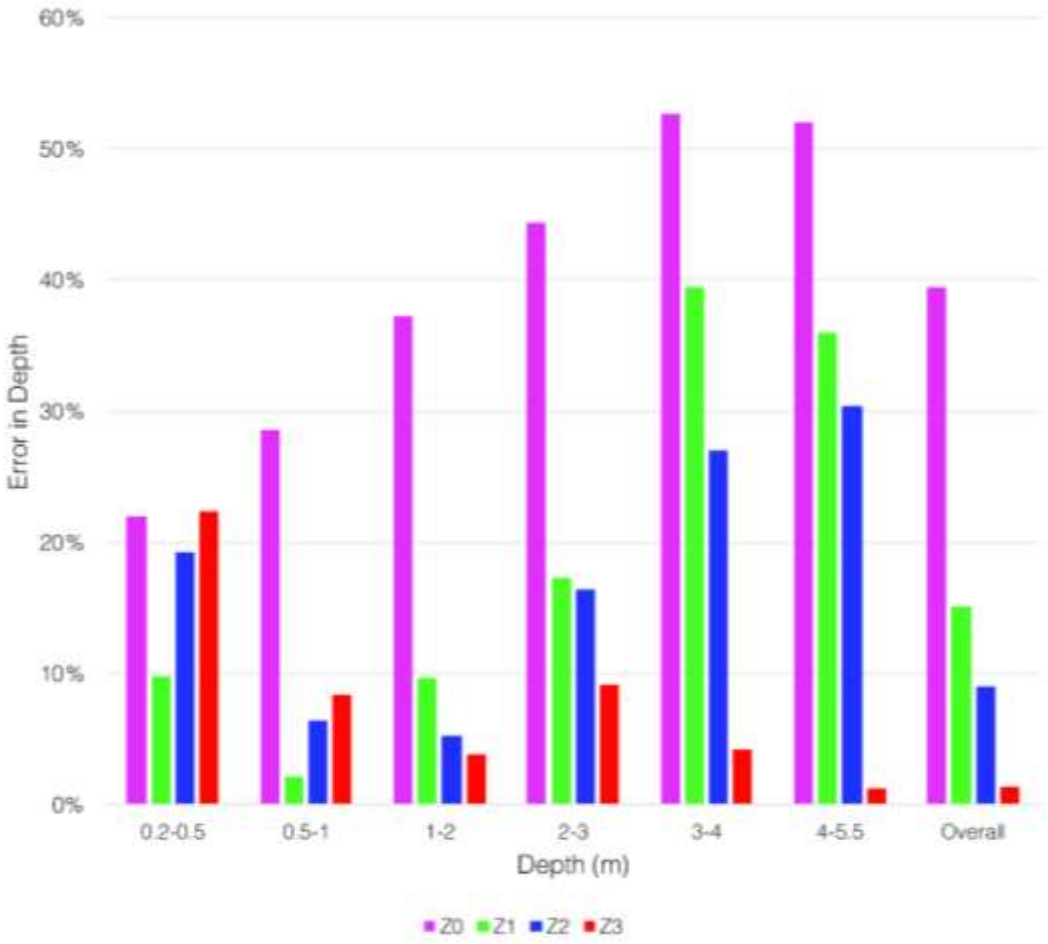

fig. 8 - Error (%) in depth after initial run (Z0), after 1st iteration (Z1), after 2nd iteration (Z2) and after last iteration (Z3), for different depths ranges.

3.2 Implementation

3.2.1 Data Collection and Processing

Implementation of the algorithm took place in Agia Napa ancient anchorage site, in support of a new marina construction. Two flights were conducted with average flying height of 207m collecting 159 photos in total with 7cm image resolution, covering an area of about 1.34km^2. Using the standard photogrammetric process, the aerial imagery and GCPs were used for aerial triangulation and an initial provisional DEM (fig. 9) was created, followed by orthophoto creation and mosaicking to produce an initial orthophotomap (fig. 10) of the area. The GCPs were used to georeferenced the final products, achieving accuracy of 6.3cm (1.05 pix).

The aerial photos and initial DEM, along with the camera calibration parameters and exterior orientation were used to run the algorithm and produce a new set of photos, partially corrected from refraction. The new photos were then used to rerun the aerial triangulation and produce a new, more accurate DEM. This iterative process was repeated three times, based on the algorithm verification results at the Amathunta case study. From the final DSM, Orthophotographs were created to produce and export the final Orthophotomap.

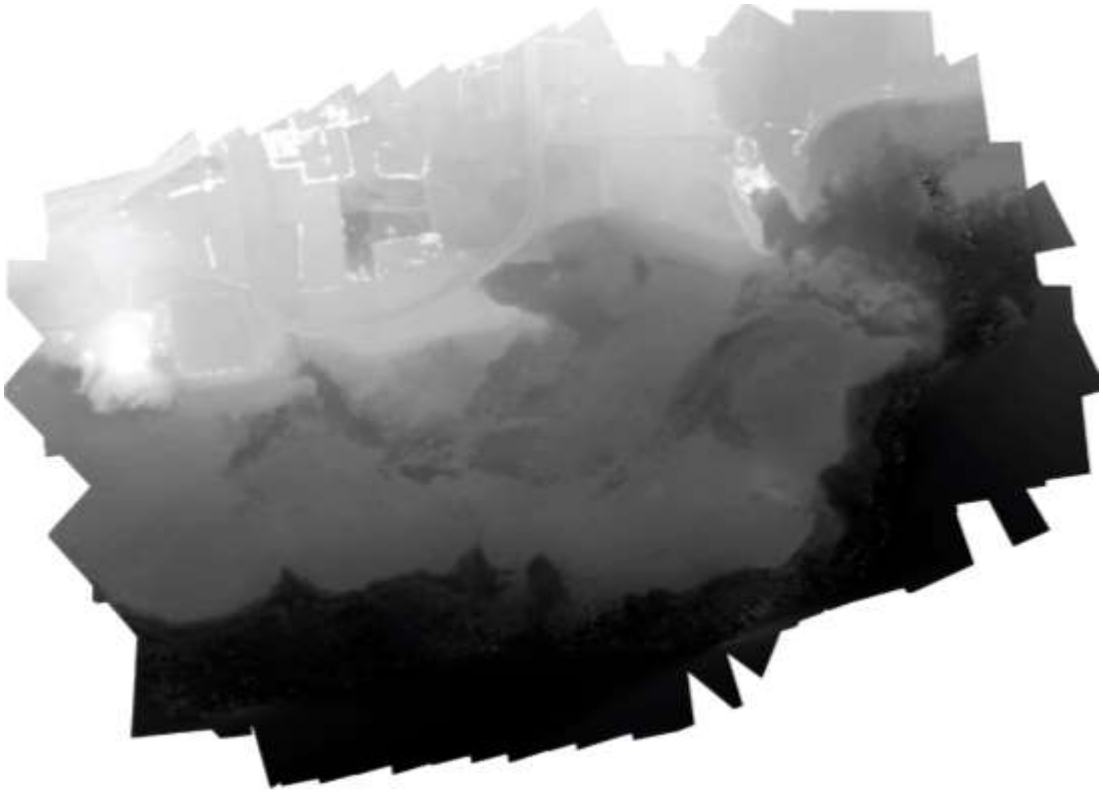

fig. 9 - Initial Digital Elevation Model of Agia Napa ancient anchorage site.

fig. 10 - Orthophotomap of Agia Napa ancient anchorage site created from initial depths, with GCPs (yellow triangles) overlaid with the marina construction plan.

3.2.2 Results

The results of the Agia Napa case study where the algorithm was implemented can be seen in fig. 11. Bathymetric contours were extracted from the initial provisional DEM as well as from the final more accurate DEM produced after the third iteration. In fig. 11 the orthophoto of Agia Napa coast is overlaid with the initial (red) and corrected (red) bathymetric contours. The contours extracted from the provisional DEM show the sea bed to be more shallow that what it actually is. After the correction, the contours show the same sea bed area to be deeper which is much closer to the reality, without the effect of refraction.

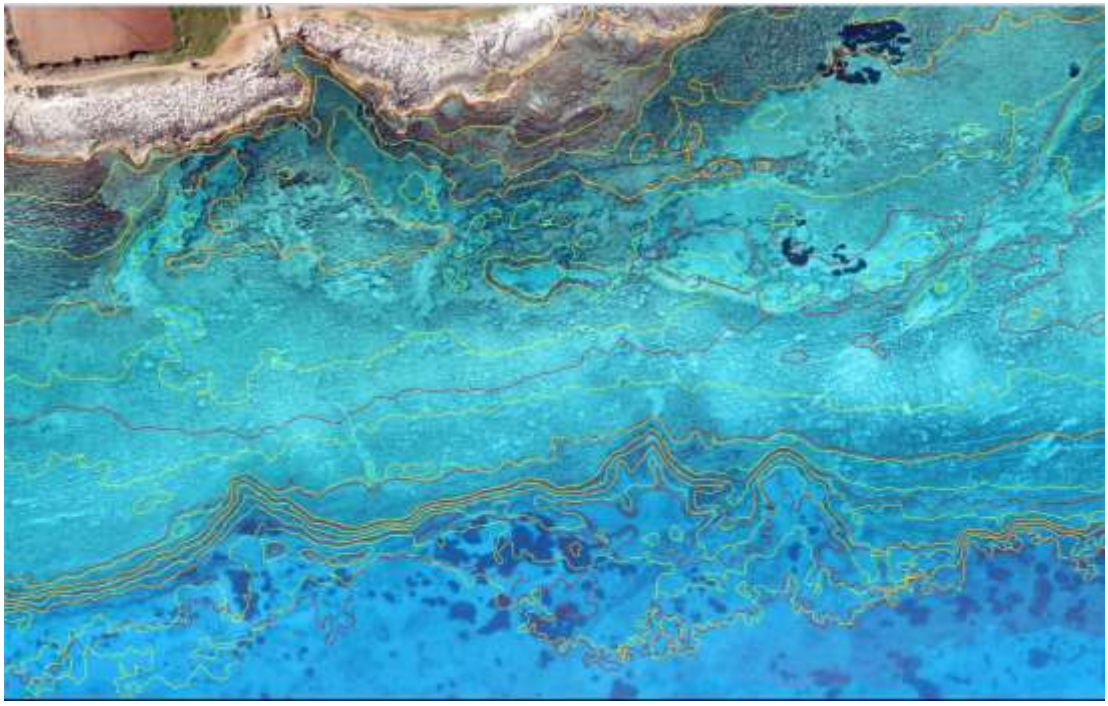

fig. 11 - Agia Napa ancient anchorage site bathymetric contours before (red) and after (yellow) the refraction corrections.

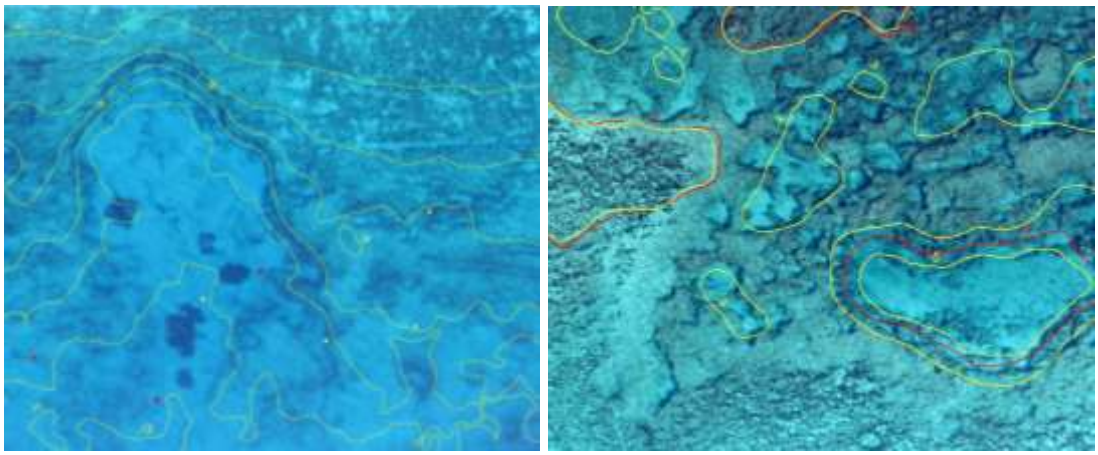

(a) (b)

fig. 12 – Detail of Detail of the Agia Napa ancient anchorage site (a) with corrected bathymetric contours and locations of ancient anchors and amphora fragments, and (b) with bathymetric contours before (red) and after (yellow) the refraction corrections.

Fig. 12 shows details of the sea bottom at the Agia Napa coast, an indication of the high resolution imagery that can be collected from UAVs in clear shallow waters. When produced from such high resolution imagery, orthophotomaps can provide archaeological information of significant detail, even underwater, relating both overwater structures with underwater ones or finds.

4. Conclusions

A new iterative methodology and corresponding algorithm have been presented to correct the problems of water refraction in aerial photos over coastal sites. The methodology is iterative, because in order to correct the refraction, the depth of the water must be known. As the water depth is also an unknown along with the amount of refraction, the process can only be iterative. Since the refraction effect is more prominent in lower flying heights, the proposed methodology is more important if more details of the sea bottom are needed, such as in archaeological surveys. The most important aspect of this work is that is allows a unified, seamless and accurate DEM and orthophoto over coastal areas. As a by-product, one may use the method to accurately calculate depth of up to 13m approximately. This option impossible using stereo vision, previously. Without proper DSM available, creation of a correct orthophoto map of the sea bottom was also impossible. There are of course shortcomings as well. The sea surface is considered flat and of same altitude. The depth extraction is limited by water visibility, which might not always be optimal. The process is iterative, hence more time consuming than traditional DSM and orthophoto creation. This work has proven that refraction severely affects depth estimation, and if not taken into consideration severe depth miscalculation will occur. At the same time this work provides a valid and accurate alternative for depth extraction and orthophoto creation in coastal sites, a possibility which previously was not an option at all.

5. Acknowlegments

The authors would like to express their gratitude to the Honor Frost Foundation for funding this project, to the Department of Land and Surveys for providing the Lidar bathymetric points, the Cyprus Department of Antiquities……..

6. References

Fryer, J. F., 1983. Photogrammetry through shallow water. Australian Journal of Geodesy, Photogrammetry and Surveying, 38: 25-38.

Georgopoulos, A. and Agrafiotis, P., 2012. Documentation of a submerged monument using improved two media techniques. In Virtual Systems and Multimedia (VSMM), 2012 18th International Conference on (pp. 173-180). IEEE.

Georgopoulos, A., Skarlatos, D. A novel method for automating the checking and correction of digital elevation models using orthophotographs. Photogrammetric Record, 18(102):156-163.

Karara, H. M., 1972. Simple cameras for close-range applications. Photogrammetric Engineering, 38(5): 447-451.

Masry, S. E. and MacRitchie, S., 1980. Different considerations in coastal mapping. Photogrammetric Engineering and Remote Sensing, 46(4): 521-528.

Norvelle, F. R., 1994. Using iterative orthophoto refinements to generate and correct digital elevation models. Proceedings: Mapping and remote sensing tools for the 21st century. American Society for Photogrammetry and Remote Sensing, Bethesda, Maryland, USA. 250, pages:134-142.

Norvelle, F. R., 1996. Using iterative orthophoto refinements to generate and correct digital elevation models (DEM's). Digital Photogrammetry: An addendum to the Manual of Photogrammetry. American Society for Photogrammetry and Remote Sensing. Bethesda, Maryland, USA. 247 pages:151-155.

Shan, J., 1994. Relative orientation for two-media photogrammetry. Photogrammetric Record, 14(84): 993-999.

Slama, C. C., 1980. Manual of Photogrammetry, Fourth edition, American Society of Photogrammetry, Falls Church, Virginia, 1056 pages.

Westaway, R.M., Lane, S.N. and Hicks, D.M., 2001. Remote sensing of clear-water, shallow, gravel-bed rivers using digital photogrammetry. Photogrammetric Engineering & Remote Sensing, 67(11): 1271-1281.

Whittlesey, J., 1975. Elevated and Airborne Photogrammetry and Stereo Photography, in Photography an Archaeological Research. edited by Elmer Harp JNR., Univ. of New Mexico Press, Albuquerque, pp.223-258.